

Comparative functional analysis of full-length and N-terminal fragments of phytochrome C, D and E in red light-induced signaling

Éva Ádám^{1,*}, Stefan Kircher^{2,*}, Peng Liu³, Zsuzsanna Mérai², Nahuel González-Schain⁴, Maximilian Hörner⁵, András Viczián¹, Elena Monte⁴, Robert A. Sharrock³, Eberhard Schäfer^{2,5} and Ferenc Nagy^{1,6}

¹Institute of Plant Biology, Biological Research Centre, Temesvári krt.62., H-6726, Szeged, Hungary; ²Institute of Botany, University of Freiburg, Schänzlestrasse 1, D-79104, Freiburg, Germany; ³Department of Plant Sciences and Plant Pathology, Montana State University, Bozeman, MT 59717, USA; ⁴Departament de Genètica Molecular, Center for Research in Agricultural Genomics (CRAG) CSIC-IRTA-UAB-UB, Campus Univ. Autònoma de Barcelona, Bellaterra, 08193, Barcelona, Spain; ⁵BIOSS Center for Biological Signalling Studies, University of Freiburg, Schänzlestrasse 18, D-79104, Freiburg, Germany; ⁶Institute of Molecular Plant Science, School of Biological Sciences, University of Edinburgh, Edinburgh, EH9 3JH, UK

Summary

- Phytochromes (phy) C, D and E are involved in the regulation of red/far-red light-induced photomorphogenesis of *Arabidopsis thaliana*, but only limited data are available on the mode of action and biological function of these lesser studied phytochrome species.
 - We fused N-terminal fragments and/or full-length phyC, D and E to YELLOW FLUORESCENT PROTEIN (YFP), and analyzed the function, stability and intracellular distribution of these fusion proteins *in planta*.
 - The activity of the constitutively nuclear-localized homodimers of N-terminal fragments was comparable with that of full-length PHYC, D, E-YFP, and resulted in the regulation of various red light-induced photomorphogenic responses in the studied genetic backgrounds. PHYE-YFP was active in the absence of phyB and phyD, and PHYE-YFP controlled responses, as well as accumulation, of the fusion protein in the nuclei, was saturated at low fluence rates of red light and did not require functional FAR-RED ELONGATED HYPOCOTYL1 (FHY-1) and FHY-1-like proteins.
 - Our data suggest that PHYC-YFP, PHYD-YFP and PHYE-YFP fusion proteins, as well as their truncated N-terminal derivatives, are biologically active in the modulation of red light-regulated photomorphogenesis. We propose that PHYE-YFP can function as a homodimer and that low-fluence red light-induced translocation of phyE and phyA into the nuclei is mediated by different molecular mechanisms.

Author for correspondence:

Éva Ádám

Tel: +36 62 599717

Email: adam.eva@brc.mta.hu

Received: 13 March 2013

Accepted: 12 May 2013

New Phytologist (2013)

doi: 10.1111/nph.12364

Key words: nuclear body formation, nuclear translocation, photomorphogenesis, photoreceptor, phytochrome E.

Introduction

Plants are sessile organisms and must adapt to changes in their environment. Light is an important environmental factor, which not only provides energy for photosynthesis, but also regulates the growth and development of plants throughout their entire life cycle. To monitor changes in their ambient light environment, plants have evolved a number of photoreceptors, including the UVB-sensing photoreceptor UVB-RESISTANCE 8 (Rizzini *et al.*, 2011), the blue/UVA-monitoring cryptochromes, phototropins, the family of Zeitlupe/FKF1/LKP2 proteins (Demarsy & Fankhauser, 2009; Yu *et al.*, 2010) and the red (R)/far-red (FR) light-absorbing phytochromes (Nagy & Schäfer, 2002). Plants contain multiple forms of phytochromes; there are five genes in *Arabidopsis thaliana* encoding phytochromes (*PHYA–PHYE*).

*These authors contributed equally to this work.

These photoreceptors form two functionally distinct groups, designated as type I and type II phytochromes. Type I phyA plays an important role in the transition from heterotrophic to phototrophic growth, that is, in seedling establishment, which is one of the most critical stages of the plant life cycle. Accordingly, it has been shown that phyA is the primary photoreceptor for very low-fluence responses (VLFR) in a broad spectrum of wavelengths and for high-irradiance responses in continuous FR light (Neff & Chory, 1998). In contrast with other phys, phyA exists only as a homodimer (Sharrock & Clack, 2004). Type II phytochromes regulate R/FR photoreversible low-fluence responses (Rockwell & Lagarias, 2006); phyB is the most prominent type II phytochrome. *phyB* null mutants display very characteristic deficiencies in R/FR reversible responses and in shade avoidance responses (Reed *et al.*, 1993; Lorrain *et al.*, 2008), whereas phenotypes of *phyC*, *phyD* and *phyE* null mutants are more subtle (Aukerman *et al.*, 1997; Devlin *et al.*, 1998; Monte *et al.*, 2003).

	Journal Name	N	P	H
		12364/2013-15307		
	Manuscript No.	12364/2013-15307		
		Dispatch: 6.6.13	Journal: NPH	CE: Réka S.
	Author Received:	No. of Pages: 11	Journal: NPH	CE: Réka S.
		PI: Páramita		

1 Homodimers of phyB (Wagner *et al.*, 1996) and phyD (Clack
2 *et al.*, 2009) have been observed in wild-type (WT) and over-
3 expressing lines, and it was assumed until recently that type II
4 phys exist only as homodimers, similar to phyA. Two recent
5 papers (Sharrock & Clack, 2004; Clack *et al.*, 2009), however,
6 have provided compelling evidence that phyB and phyD hetero-
7 dimerize with each other, phyC and phyE form obligate hetero-
8 dimers with phyB and phyD *in planta*, and these heterodimers
9 can bind PHYTOCHROME INTERACTING FACTOR 3
10 (PIF3), similar to homodimers of phyB. These data suggest a
11 possible novel mechanism by which phyC, phyD and phyE con-
12 tribute to the fine tuning of phyB-mediated physiological
13 responses. Molecular analysis of PHYA-GREEN FLUORES-
14 CENT PROTEIN (GFP)- and PHYB-GFP-controlled signaling
15 cascades has demonstrated that light in a quality- and quantity-
16 dependent fashion regulates nucleo/cytoplasmic partitioning of
17 phys (Kircher *et al.*, 1999, 2002; Yamaguchi *et al.*, 1999). The
18 same authors noticed that phyA- and phyB-GFP fusion proteins
19 localized in the nucleus are not distributed evenly in the nucle-
20 oplasm, but are associated with specific subnuclear structures,
21 termed speckles, nuclear bodies (NBs) or photobodies. As for
22 phyB, it has been shown that short exposure to R light induces
23 the formation of transiently appearing phyB NBs (termed early
24 NBs), whereas extended irradiation promotes the formation of
25 more stable phyB-associated NBs, also called late NBs (for a
26 recent review, see Van Buskirk *et al.*, 2012). Subsequent work has
27 demonstrated that phyA does not contain an authentic nuclear
28 localization signal (NLS), and it was shown that the nuclear
29 import of phyA is mediated by the FAR-RED ELONGATED
30 HYPOCOTYL 1/FHY-1 LIKE (FHY1/FHL) proteins
31 (Hiltbrunner *et al.*, 2005, 2006; Fankhauser & Chen, 2008;
32 Pfeiffer *et al.*, 2009). The molecular machinery mediating the
33 nuclear import of phyB is less well understood. It has been
34 reported (Chen *et al.*, 2005) that a short domain within the PAS-
35 PAS region of the C-terminal part of phyB contains an intrinsic
36 NLS that mediates nuclear import, and it has been postulated
37 that R light-induced conformational change of the C-terminal
38 domain facilitates the interaction of phyB with the import
39 machinery. However, more recently, it has been demonstrated
40 that phyB does not possess a functional NLS motif, and that
41 PIF3 promotes light-regulated nuclear import of the photorecep-
42 tor *in vitro* and is also required for translocation of PHYB-GFP
43 into the nucleus during the early phase of the dark-to-light transi-
44 tion *in planta* (Pfeiffer *et al.*, 2012). In contrast with phyB, the
45 mechanism and identity of the factors involved in translocating
46 cytosolic phyC, phyD and phyE into the nucleus remain to be
47 elucidated.

48 It has been shown that nuclear localized dimers of short N-ter-
49 minal PHYB fragments can complement phyB-deficient mutants
50 (Matsushita *et al.*, 2003; Oka *et al.*, 2004; Palágyi *et al.*, 2010).
51 These data indicated that the N-terminal fragment of phyB, con-
52 sisting of the GAF and PHY domains, is sufficient to control and
53 launch signaling cascades that underlie many aspects of R/FR-
54 regulated photomorphogenesis. In contrast with phyB, homodi-
55 mers of the N-terminal fragment of phyA localized in the nucleus
56 are inactive in launching phyA-controlled signaling (Wolf *et al.*,

2011; Viczián *et al.*, 2012), whereas no data are available to prove
whether N-terminal fragments of phyC, phyD and phyE are
functional or can substitute to any extent the function of the
native photoreceptors. In this work, we have investigated the bio-
logical activity of full-length and N-terminal fragments of
PHYC, PHYD and PHYE fused to the YELLOW FLUORES-
CENT PROTEIN (YFP). Our data show that homodimers of
the N-terminal fragments of these phytochromes are biologically
active, they complement specific mutants lacking phyC, phyD
and phyE, and the nuclear localization of these fusion proteins is
necessary to launch efficient signaling. Moreover, we demonstrate
that homodimers of full-length PHYE-YFP are imported into the
nucleus in an R light-induced fashion, this process is induced and
saturated at low fluence rates of R light, and translocation of
phyE-YFP into the nucleus does not require heterodimerization
with phyB and/or phyD.

Materials and Methods

Cloning of the constructs

Full-length *PHYC*, *D* and *E* cDNA fragments were subcloned
from the *35S:PHYC,D,E-GFP* pPCV plasmids (Kircher *et al.*,
2002) into the *35S:YFP-NOS3'* pPCV812 (*PHYC*) or *35S:YFP-
NOS3'* pPCVB812 (*PHYD*, *PHYE*) vectors as *Bam*HI-*Ehe*I
(*PHYC*) and *Sma*I-*Ehe*I (*PHYE*, *PHYD*) fragments. The creation
of the *35S:YFP-DD-NLS/NES* pPCV812 plasmid vectors has
been described elsewhere (Pfeiffer *et al.*, 2009; Wolf *et al.*, 2011).
The cDNA fragments encoding the N-terminal domain of Ara-
bidopsis *PHYC*, *D* and *E* were amplified by polymerase chain
reaction and cloned into the *35S:YFP-DD-NLS/NES* pPCV812
vectors. *35S:PHYA-YFP* has been described by Bauer *et al.*
(2004). DNA oligonucleotides used in the construction of
recombinant genes are listed in Supporting Information
Table S1. The final constructs were verified by sequencing and
introduced into *Agrobacterium tumefaciens* GV3101.

Plant transformation and regeneration of transgenic lines

Arabidopsis thaliana (L.) plants were transformed by the
Agrobacterium-mediated floral dip method (Clough & Bent,
1998). Details of the raised transgenic lines and the mutant back-
grounds used are given in Table S2. From each of these transfor-
mations, transgenic seedlings expressing the fusion proteins were
selected by their resistance to hygromycin or Basta, and grown to
maturation in the glasshouse (for details, see Bauer *et al.*, 2004).
Independent homozygous lines expressing one copy of the trans-
gene were selected for further analysis.

Seedling and plant growth conditions and growth measurements

For hypocotyl length measurements, seeds were sown on four lay-
ers of filter paper and imbibed in water for 48 h at 4°C. For coty-
ledon area measurements, seeds were placed on Murashige and
Skoog (MS) medium without sucrose. Cold-treated seeds were

then irradiated with white light for 3 h at 22°C to induce seed germination, and transferred to dark for an additional 18 h at 22°C. The plates were then placed under various light conditions for 4 d or otherwise, specified in the figure legends. Seedlings were placed horizontally on the surface of agar medium and scanned ($n=50$). Images of scanned seedlings were analyzed using MetaMorph Software (Universal Imaging, Downingtown, PA, USA). Hypocotyl length values, measured at different fluences of light, were normalized to the corresponding dark-grown hypocotyl length to reflect solely the light-dependent regulation.

Flowering time measurement

Seeds were sown in water and incubated for 2 d in the dark at 4°C. They were then placed on the surface of soil and transferred to short-day conditions (SD, 8 h white light : 16 h dark at 22°C). Light sources were fluorescent (cool-white) tubes producing a fluence rate of $60 \mu\text{mol m}^{-2} \text{s}^{-1}$. The flowering time was recorded as the number of rosette leaves at the time at which inflorescences reached a height of 1 cm ($n=40$).

Epifluorescence microscopy

Seeds were sown on a four-layer filter paper and imbibed in water in the dark for 48 h at 4°C. Cold-treated seeds were then transferred to 25°C and irradiated with 18 h of white light to induce homogeneous germination, and grown for additional days in the dark. Six-day-old dark-grown seedlings were then subjected to various light treatments, as described in the text. The standard epifluorescence microscopy set-up and observation techniques have been described previously (Bauer *et al.*, 2004; Viczián & Kircher, 2010; Sokolova *et al.*, 2012). For semiquantitative epifluorescence microscopy, etiolated seedlings were irradiated for 6 h with R light at the fluence rates given in the figure legends. Using an Axioplan microscope (Zeiss, Germany) equipped with a CoolSnap HQ camera (Photometrics, USA), 12-bit TIFF images, not containing saturated pixels, were taken of nuclei in epidermal cells of hypocotyls. In order to minimize the effect of the microscopic light, images were taken within the first 120 s after the onset of excitation light. Adjusted and identical exposure times and excitation light intensity settings were applied throughout the analysis of each genotype. The average intensity of nuclear pixels was calculated using ImageJ software (National Institutes of Health, USA), including the subtraction of background signals in each image. The mean value of the data obtained from at least 25 independent nuclei was normalized to the corresponding dark control. For each genotype, three independent biological replica experiments were performed.

Plant protein extraction and western blot hybridization

Seedling protein extracts were prepared in extraction buffer (50 mM Tris, pH 8.0, 150 mM NaCl, 0.1% NP-40), as described previously (Sharrock & Clack, 2004). Proteins were fractionated on 6% sodium dodecylsulfate-polyacrylamide gel electrophoresis (SDS/PAGE) gels and transferred to Hybond-ECL membranes

(GE Healthcare). Membranes were blocked overnight at 4°C with blocking buffer (5% non-fat dry milk, 0.2% Tween 20 in TBS-T buffer, pH 7.6). Membranes were probed in blocking buffer containing the following primary monoclonal antibodies: anti-phyC C11 and C13, anti-phyD 2C1, and anti-phyE 7B3 (Hirschfeld *et al.*, 1998). After three washes with TBS-T buffer, chemiluminescent detection of primary antibodies was performed with horseradish peroxidase-conjugated secondary antibody and Supersignal West Pico reagents (Thermo Fisher Scientific). Total protein was analyzed by the Bio-Rad Protein Assay. For native gel electrophoresis, 7-d-old seedlings grown under the described light conditions were ground at 0°C under dim green safe light at a 1 : 1 weight : volume ratio in non-denaturing extraction buffer (25 mM Tris-HCl, pH 7.5, 10 mM NaCl, 5 mM EDTA) containing Complete EDTA-free Protease Inhibitor Cocktail (Roche Diagnostics, Indianapolis, IN, USA), and the extracts were centrifuged for 3 min at 4°C. Proteins were separated on 4–20% gradient PAGE gels in Tris/borate/EDTA buffer for 40 h at 4°C. Gel blotting was the same as for SDS-PAGE gels, and blots were probed with anti-GFP antibody GF28R (Thermo Fisher Scientific). Secondary antibodies coupled to horseradish peroxidase (Bio-Rad) were used according to the manufacturer's recommendations.

Analysis of transcript levels

Seeds were surface sterilized and plated onto MS medium, stratified at 4°C in the dark for 3 d, and exposed to white light for 3 h to induce germination. Subsequent growth conditions and light inductions were carried out as described in the corresponding figure legends. RNA samples were prepared from whole seedlings using RNeasy Miniprep Kits (Qiagen) according to the manufacturer's instructions, and DNA was removed by DNase I treatment. cDNA was synthesized from 1 μg of total RNA using the Revert Aid First Strand cDNA Synthesis Kit (Fermentas). Real-time reverse transcription-polymerase chain reaction (RT-PCR) analysis was carried out with a 7500Real-Time PCR System with SYBR Green JumpStart TaqReadyMix (Sigma). The expression levels were normalized to the expression of *TUBULIN2/3*. The experiments were performed at least three times, and a representative dataset is presented. The primers used in qRT-PCRs are listed in Table S1.

Accession numbers

PHYB, AT2G18790; *PHYC*, AT5G35840; *PHYD*, AT4G16250; *PHYE*, AT4G18130; *FHY1*, AT2G37678; *FHL*, AT5G02200; *PRR9*, At2g46790; *CAB2*, At1g29920; *ELIP1*, AT3G22840; *EXPANSIN5*, AT3G29030; *EXPANSIN9*, AT5G02260; *BBX23*, AT4G10240; *HB4*, AT2G44910; *TUBULIN2/3*, AT5G62690.

Results

To test whether homodimers of N-terminal fragments of phyC, phyD and phyE, similar to those of phyB, can launch R

light-induced signaling, we constructed chimeric genes consisting of the N-terminal domains of *PHYC*, *PHYD* and *PHYE* fused to the *YFP* reporter under the control of the viral 35S promoter. These domains were selected on homology to the N-terminal 1–651-amino-acid region of *PHYB* (Fig. S1). Appropriate dimerization and targeted, constitutive, subcellular localization were achieved by the addition of the leucine-zipper domain of the CPRF transcription factor (DD) and the SV 40 NLS peptide or nuclear exclusion signal (NES), as described by Palágyi *et al.* (2010) and Wolf *et al.* (2011). The domain structures of the various fusion proteins are shown in Fig. S1. The synergistic and, in some cases, antagonistic action of phytochrome species makes the elucidation of the roles of minor family members in single mutants difficult. Therefore, we used double-, triple- or quadruple-mutant combinations showing characteristic deficient phenotypes to assess the functions of these fusion proteins. We regenerated 15 independent transgenic lines for each construct and used quantitative western blot hybridization to select lines which expressed the individual full-length *PHYC*-YFP, *PHYD*-YFP and *PHYE*-YFP, and their N-terminal derivative fusion proteins, approximately at the same or, at least, comparable levels. The genetic backgrounds of the transgenic lines and the expression levels of the various fusion proteins relative to their

endogenous *phyC*, *phyD* and *phyE* counterparts are shown in Tables S2 and S3, respectively.

Homodimers of *phyC* N-terminal fragments localized in the nucleus are functional in regulating R light-induced signaling

The selected transgenic *phyC/phyD* mutant lines over-expressed the *PHYC*-YFP *c.* two-fold, whereas the expression level of the *PHYC602*-YFP-DD-NLS and *PHYC602*-YFP-DD-NES fusion proteins was *c.* 40% or 70% of the endogenous *phyC*, respectively (Table S3). *PHYC*-YFP fully, and the *PHYC602*-YFP-DD-NLS fusion protein partially, restored R light-induced hypocotyl growth inhibition of the *phyC/phyD* mutant (Fig. 1a). R light-induced expansion of the cotyledon area of the mutant was also restored (Fig. 1b) and, in this case, *PHYC*-YFP-expressing seedlings exhibited a weak over-expression phenotype, whereas the *PHYC602*-YFP-DD-NLS seedlings displayed a nearly fully complemented phenotype. These fusion proteins also restored *phyC* function in regulating the flowering time under SD conditions (Fig. 1c). By contrast, the *PHYC602*-YFP-DD-NES photoreceptor was biologically inactive in all responses tested, as the *PHYC602*-YFP-DD-NES-expressing seedlings invariably

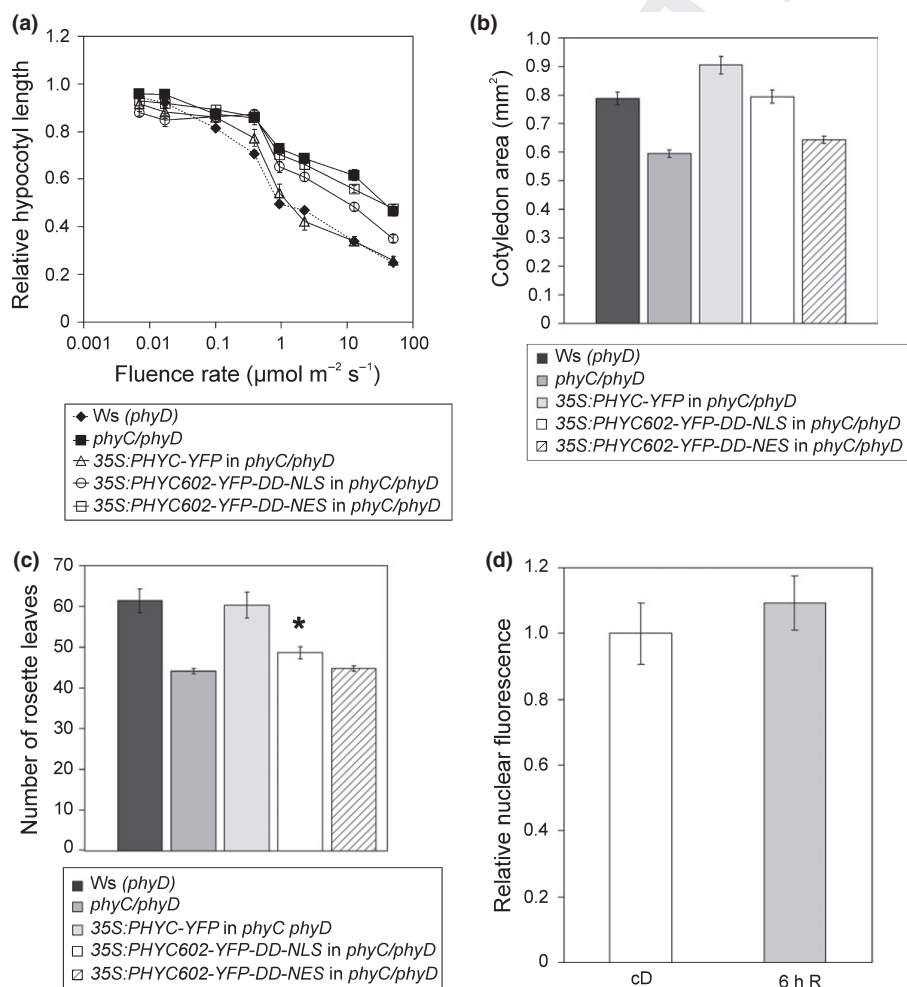


Fig. 1 *PHYC*-YFP and *PHYC602*-YFP-DD-NLS complement photomorphogenic and flowering time phenotypes of the *phyC/phyD* mutant of *Arabidopsis thaliana*. (a) Fluence response curves for the inhibition of hypocotyl elongation in red (R) light. Student's two-tailed heteroscedastic *t*-test shows a significant difference between *phyC/phyD* and 35S:*PHYC602*-YFP-DD-NLS ($P < 0.01$ at $12.8 \mu\text{mol m}^{-2} \text{s}^{-1}$ and $P < 0.001$ at $50 \mu\text{mol m}^{-2} \text{s}^{-1}$). (b) Expansion of cotyledon area of 4-d-old seedlings grown in constant R light (cR) ($25 \mu\text{mol m}^{-2} \text{s}^{-1}$). (c) Flowering time in short-day photoperiod. Asterisk indicates statistically significant difference between *phyC/phyD* and 35S:*PHYC602*-YFP-DD-NLS expressing plants, as determined by Student's two-tailed heteroscedastic *t*-test (*, $P < 0.05$). (d) Nuclear accumulation of *PHYC*-YFP is not modulated by 6 h R light ($25 \mu\text{mol m}^{-2} \text{s}^{-1}$) in transgenic *phyC/phyD* mutant. cD, etiolated control. Error bars indicate \pm SE. All experiments shown were repeated three times. **8**

1 displayed the original *phyC/phyD* mutant phenotype in all
2 experiments performed (Fig. 1a–c). The abundance of the native
3 *phyC* and the various PHYC-YFP fusion proteins was down-reg-
4 ulated by constant R light (cR) irradiation. Irradiation with 120 h
5 of cR light ($25 \mu\text{mol m}^{-2} \text{s}^{-1}$) reduced the level of the
6 endogenous *phyC* below the detection level (Fig. S2a), and
7 decreased the levels of all other *phyC* fusion proteins *c.* four-fold
8 (Fig. S2b).

9 Microscopic analysis of the nucleocytoplasmic distribution of
10 the various PHYC-YFP fusion proteins demonstrated that, in eti-
11 olated as well as R light-irradiated seedlings, PHYC602-YFP-
12 DD-NLS was detectable only in the nucleus (Fig. S3a–c),
13 PHYC602-YFP-DD-NES was localized exclusively in the cyto-
14 plasm (Fig. S3d–f) and PHYC-YFP was observed in both the
15 nucleus and cytoplasm in etiolated as well as in R light-irradiated
16 seedlings (Fig. S3g–i). A 5-min R light treatment induced the
17 formation of early PHYC-YFP NBs, whereas a prolonged, 24-h
18 R light treatment promoted the formation of late, stable PHYC-
19 YFP NBs. Under these conditions, we could not detect the
20 appearance of either early or late NBs associated with the truncated
21 forms of PHYC. Quantitative analysis of the fusion protein indicated that a 6-h cR light
22 treatment did not modify significantly the level of PHYC-YFP in
23 the nucleus (Fig. 1d).

24 Homodimers of *phyD* N-terminal fragments localized in the 25 nucleus restore *phyD* signaling

26 The selected transgenic *phyA/phyB/phyD* plants over-expressed
27 PHYD-YFP two-fold and the PHYD-N654-YFP-DD-NLS and
28 PHYD-N654-YFP-DD-NES fusion proteins *c.* 25 and 20-fold,
29 respectively, when compared with endogenous *phyD* (Table S3).
30 Analysis of R light-induced hypocotyl growth inhibition
31 (Fig. 2a), cotyledon expansion (Fig. 2b) and flowering time
32 (Fig. 2c) under SD conditions demonstrated that the PHYD654-
33 YFP-DD-NLS and PHYD-YFP fusion proteins were biologically
34 active. As for hypocotyl growth inhibition and cotyledon expan-
35 sion, PHYD654-YFP-DD-NLS displayed a dramatic, and
36 PHYD-YFP a moderate, over-expression phenotype when com-
37 pared with the *phyA/phyB* double null mutant (Fig. 2a,b). The
38 flowering time of the *phyA/phyB/phyD* mutant was also fully
39 restored by PHYD-YFP, whereas the PHYD654-YFP-DD-NLS-
40 expressing lines again displayed strong over-expression pheno-
41 types (Fig. 2c). The PHYD654-YFP-DD-NES fusion protein
42 was biologically inactive, as transgenic seedlings/plants invariably
43 displayed the original *phyA/phyB/phyD* mutant phenotype for all
44 responses tested. The abundance of the native *phyD* and the vari-
45 ous PHYD-YFP fusion proteins was not affected significantly by
46 cR light treatment. Irradiation with cR light ($25 \mu\text{mol m}^{-2} \text{s}^{-1}$)
47 did not modify the level of either the native *phyD* (Fig. S4a) or
48 the full-length and truncated PHYD-YFP fusion proteins
49 (Fig. S4b).

50 The nucleocytoplasmic distribution of the various PHYD-
51 YFP fusion proteins was analyzed as described for the various
52 PHYC-YFP fusion proteins. PHYD654-DD-YFP-NLS was visi-
53 ble in the nucleus under all conditions tested, whereas

PHYD654-DD-YFP-NES was detected exclusively in the cyto-
plasm, and these truncated proteins never associated with NBs
(Fig. S5a–c and d–f, respectively). PHYD-YFP was clearly visible
in the nucleus in etiolated seedlings, and R light treatments did
not affect the amount of photoreceptor localized in the nucleus
or induce the formation of early/late PHYD-YFP-containing
NBs (Fig. S5h–i). Quantitative analysis of the accumulation of
PHYD-YFP in the nucleus corroborated these observations
(Fig. 2d).

54 Homodimers of *phyE* N-terminal fragments localized in the 55 nucleus are capable of signaling in red light

56 The selected transgenic *phyA/phyB/phyE* plants expressed the
PHYE-YFP and PHYE593-YFP-DD-NLS fusion proteins eight-
to ten-fold and the PHYE593-YFP-DD-NLS protein *c.* three- to
four-fold more strongly than the native *phyE* (Table S3) Analysis
of R light-induced inhibition of hypocotyl growth and cotyledon
expansion demonstrated that, with the exception of PHYE593-
YFP-DD-NES, these fusion proteins efficiently complemented
the *phyA/phyB/phyE* mutant, and even displayed characteristic
over-expression phenotypes when compared with *phyA/phyB*
mutants (Fig. 3a,b). These responses were induced at very low
fluence rates ($> 0.001 \mu\text{mol m}^{-2} \text{s}^{-1}$) and saturated at low flu-
ence rates ($0.01 \mu\text{mol m}^{-2} \text{s}^{-1}$). Transgenic plants expressing
nuclear localized homodimers of N-terminal fragments of PHYB,
but not the full-length PHYB, were similarly hypersensitive at
low fluences of R light (Oka *et al.*, 2004). The same fusion pro-
teins, again with the exception of the truncated PHYE593-YFP-
DD-NES, complemented the flowering time of the *phyA/phyB/*
phyE triple mutant (Fig. 3c). The abundance of the native *phyE*
and the various PHYE-YFP fusion proteins was down-regulated
by irradiation with cR light ($25 \mu\text{mol m}^{-2} \text{s}^{-1}$). Exposure to
120 h cR light reduced the abundance level of the native *phyE*
c. two-fold (Fig. S6a) and that of the full-length and truncated
PHYE-YFP fusion proteins *c.* four-fold (Fig. S6b). We also ana-
lyzed the cellular distribution of the full-length and truncated
PHYE-YFP fusion proteins in this genetic background. The
PHYE593-YFP-DD-NLS fusion protein was constitutively
nuclear; its accumulation in the nucleus did not increase after
prolonged exposure to R light (Fig. S7a–c). By contrast,
PHYE593-YFP-DD-NES, as expected, was detectable only in
the cytoplasm, independent of the light conditions (Fig. S7d–f).
As for PHYE593-YFP-DD-NLS, short 5-min R light irradiation
induced the formation of early NBs, but extended R treatment
did not promote the appearance of late, stable NBs associated
with this fusion protein (Fig. S7a–c). By contrast, we could not
detect the formation of any NBs containing PHYE593-YFP-
DD-NES. The PHYE-YFP fusion protein was detectable in the
nuclei of etiolated seedlings, but a 24-h R light treatment clearly
induced its nuclear abundance. In addition, R light also induced
the appearance of early NBs, but did not promote the formation
of late, stable PHYE-YFP-associated NBs (Fig. S7g–i). Quanti-
tative analysis of the R light-induced accumulation of the
PHYE-YFP fusion protein in the nucleus corroborated these
observations (Fig. 3d).

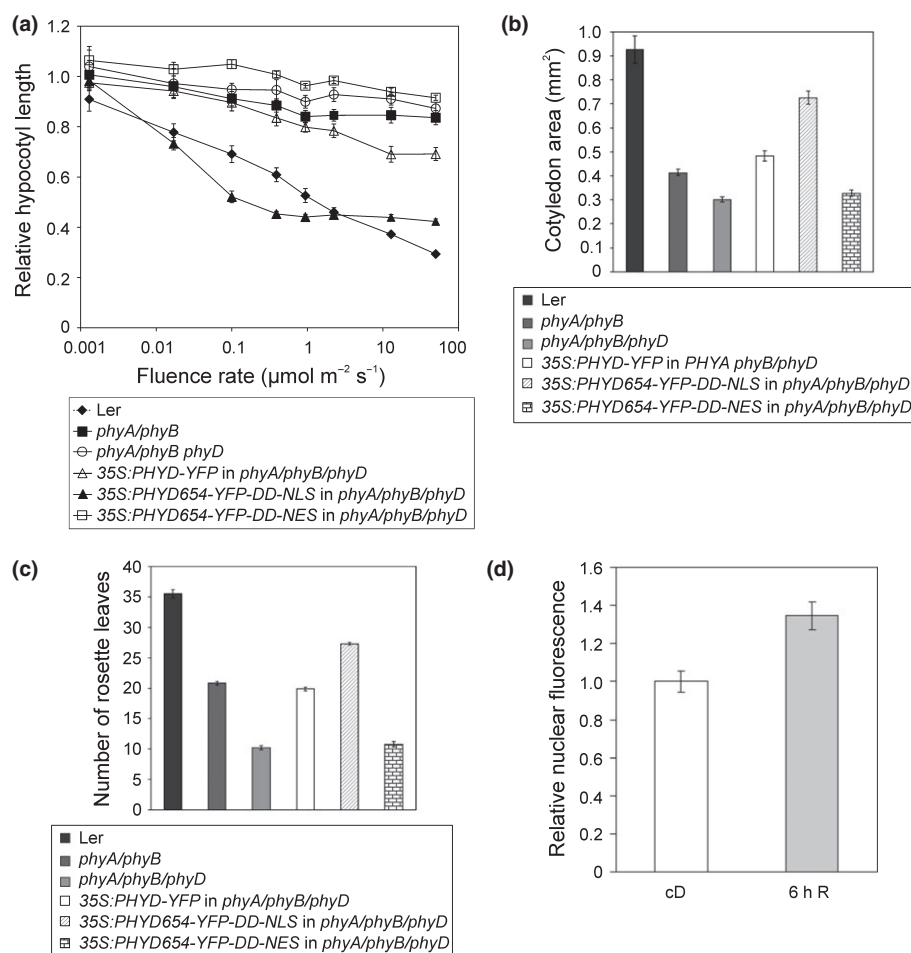


Fig. 2 PHYD-YFP and PHYD654-YFP-DD-NLS are biologically active and complement the *phyA/phyB/phyD* mutant of *Arabidopsis thaliana*. (a) Fluence rate curves for the inhibition of hypocotyl growth in red (R) light. (b) Expansion of cotyledon area of 4-d-old seedlings grown in constant R light (cR) ($25 \mu\text{mol m}^{-2} \text{s}^{-1}$). (c) Flowering time in short-day photoperiod. (d) 6 h of R light ($25 \mu\text{mol m}^{-2} \text{s}^{-1}$) does not elevate significantly the amount of PHYD-YFP in the nucleus. cD, etiolated control. Error bars indicate \pm SE. All experiments shown were repeated three times. **9**

Homodimers of PHYE-YFP are functional and imported into the nucleus at very low fluences of R light independent of *phyA*, *phyB* and *phyD*

To test to what extent the functionality of PHYE-YFP depends on *phyD*, the PHYE-YFP transgene from the *phyA/phyB/phyE* mutant was introgressed into the *phyA/phyB/phyD/phyE* quadruple null background. Analysis of R light-induced hypocotyl growth inhibition demonstrated that PHYE-YFP is functional in the absence of *phyA*, *phyB* and *phyD* (Fig. 4a). This figure also shows that seedlings expressing PHYE-YFP display a characteristic over-expression phenotype when compared with the *phyA/phyB/phyD/phyE* mutant, and the physiological response in this genetic background also saturates at $0.01 \mu\text{mol m}^{-2} \text{s}^{-1}$ fluence rate of R light, and resembles the data obtained by the analysis of PHYE-YFP function in the *phyA/phyB/phyE* triple null background (Fig. 3a). The extreme sensitivity of these PHYE-YFP responses to R light prompted us to test whether the biological activity and nuclear accumulation of PHYE are mediated by FHY1/FHL proteins, shown to be essential for the translocation of *phyA* into the nucleus. To this end, we produced PHYE-YFP-expressing transgenic *fhy1/fhl* mutant lines. Figure 4(b) illustrates that the PHYE-YFP-expressing seedlings are hypersensitive to low fluences of R light when compared with *fhy1/fhl* or Col-0

WT. Quantitative analysis of R light-induced accumulation of PHYE-YFP in the nucleus demonstrated that this process is saturated at $0.08 \mu\text{mol m}^{-2} \text{s}^{-1}$ fluence rate of R light in contrast with PHYB-GFP (Fig. 4c–d). We note that R light is ineffective in inducing the formation of early and/or late, stable PHYE-YFP NBs in the *phyA/phyB/phyD/phyE* background, whereas these nuclear structures were readily detectable in the *fhy1/fhl* mutant (Table S4). To test whether the PHYE-YFP photoreceptor functions and is imported into the nucleus as a monomer or homodimer, we analyzed total protein extracts prepared from etiolated and R light-treated seedlings by native gel electrophoresis. Our data demonstrate that the PHYE-YFP fusion protein is detected nearly exclusively as a homodimer in these extracts, and that extended irradiation with R light reduces significantly the abundance of PHYE-YFP (Fig. 4e). In addition, we show that, similar to the *phyA-201* null mutant, a short pulse of R light is not capable of inducing significant accumulation of *PRR9*, *CAB2* or *ELIP1* transcripts in transgenic *phyA/phyB/phyD/phyE* seedlings over-expressing PHYE-YFP (Fig. 5a). However, Fig. 5(b) indicates that over-expressed PHYE-YFP in the *phyA/phyB/phyE* and/or *phyA/phyB/phyD/phyE* background can restore the transcriptional regulation of *EXPANSIN5* and *9*, thought to regulate cell wall extension in an opposite fashion. Taken together, these data strongly suggest that PHYE-YFP can function as a homodimer

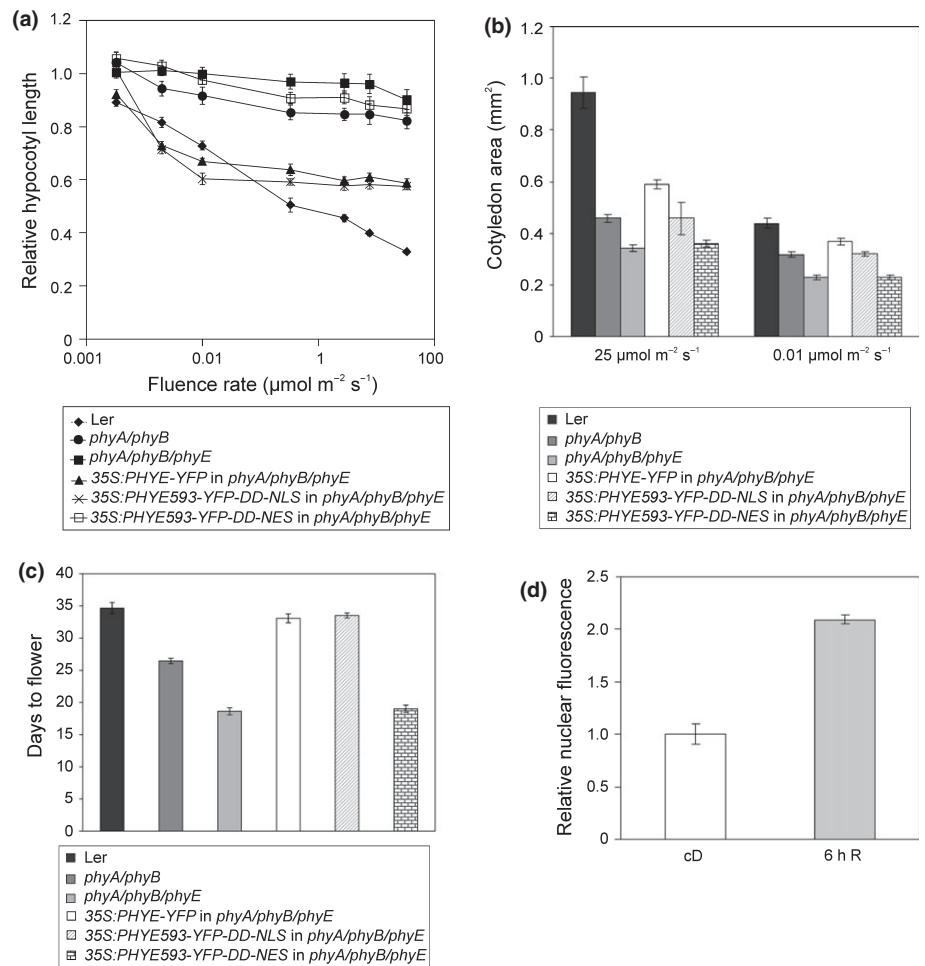


Fig. 3 Transgenic *Arabidopsis thaliana* *phyA/phyB/phyE* seedlings expressing the PHYE-YFP and PHYE593-DD-YFP-NLS fusion proteins respond to constant red (R) light (cR) irradiation. (a) Fluence response curves for the inhibition of hypocotyl elongation of 4-d-old seedlings grown in cR. (b) Cotyledon expansion after continuous exposure to 25 or 0.01 $\mu\text{mol m}^{-2} \text{s}^{-1}$ R light for 4 d. (c) Flowering time in short-day conditions. (d) 6 h of R light (25 $\mu\text{mol m}^{-2} \text{s}^{-1}$) promotes the accumulation of PHYE-YFP in the nucleus. cD, etiolated control. Error bars indicate \pm SE. All experiments were repeated three times.

10

independent of *phyB*, *phyD* and *phyA*, the nuclear import of *phyE* does not require functional *FHY1/FHL* proteins, the PHYE-controlled signaling cascade operates differently from that controlled by *phyA* at very low fluences of R light, and the formation of late, stable PHYE-YFP NBs requires functional *phyB*.

Discussion

In this work, we have demonstrated that homodimers of the N-terminal fragments of PHYC, PHYD and PHYE are biologically active and restore the photomorphogenic phenotypes of specific mutants lacking these photoreceptors. Our data show a good correlation between the expression levels and physiological activities of these truncated photoreceptors, suggesting that their C-terminal domains are dismissible for signaling. These data also indicate that import/accumulation of the photoreceptors to/in the nucleus is essential for biological activity. Moreover, our data demonstrate that exposure to R light modulates the abundance of these fusion proteins, similar to native *phyC*, *phyD* and *phyE* (Figs S2, S4, S6), and they uniformly fail to produce detectable late NBs (Figs S3, S5, S7). These observations are strikingly similar to the data reported for *phyB* N-terminal fragments (Matsushita *et al.*, 2003; Oka *et al.*, 2004; Palágyi *et al.*, 2010), but, in contrast with *phyB*, the mode of action by which PHYC, PHYD

and PHYE N-terminal fragments launch R/FR-dependent signaling is not understood. As for *phyB* and PHYB N-terminal fragments, it has been reported that they mediate light signaling by inhibiting the activity of PIFs via the release of these bHLH-type transcription factors from their DNA targets (Park *et al.*, 2012). The inhibition requires interaction between the P_{fr} form of the photoreceptor and PIFs, and it has been concluded that this interaction competes directly with DNA binding.

At present, there are no data available to demonstrate that homodimers of full-length or N-terminal fragments of PHYC, PHYD and PHYE P_{fr} can bind to PIF3 or any other PIFs, either *in vitro* or *in vivo*. In this respect, we note that the data reported by Clack *et al.* (2009) show that heterodimers of full-length *phyB/phyC* and *phyB/phyD* can be co-immunoprecipitated with PIF3. However, we should emphasize that it is highly unlikely that PHYC, PHYD and PHYE N-terminal fragments would heterodimerize with full-length *phyB* and *phyD*, and, in addition, we demonstrate in this work that full-length PHYE-YFP is functional in the absence of *phyB* and *phyD*. Thus, we conclude that, in the absence of additional molecular details, the precise mechanism underlying R/FR reversible signaling by these phytochrome species remains elusive.

Independent of the molecular mechanism governing signaling by the PHYC, PHYD and PHYE N-terminal fragments, our

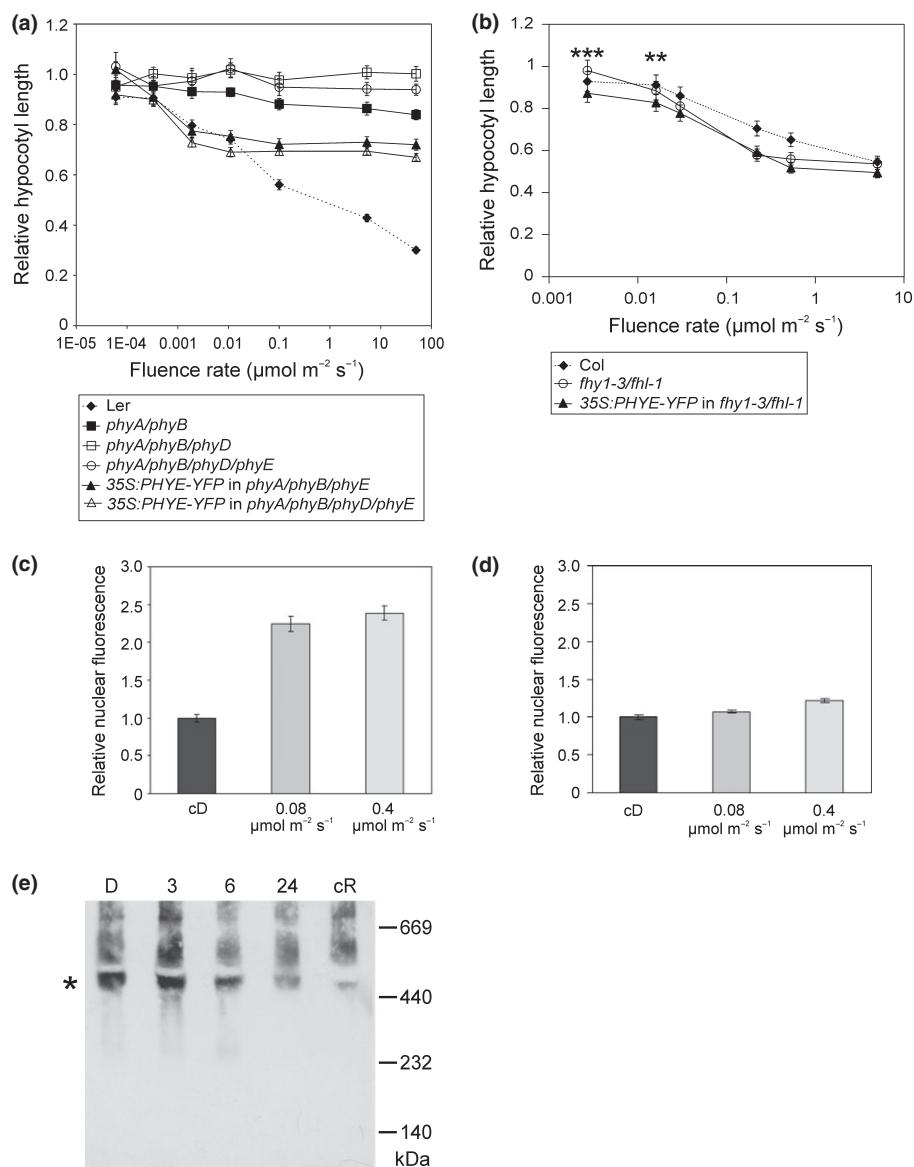


Fig. 4 PHYE-YFP is active in transgenic *Arabidopsis thaliana phyA/phyB/phyD/phyE* and in *fhy1/fhl* seedlings, accumulates in the nucleus in a red (R) light-induced fashion and forms homodimers. (a) Fluence response curves for the inhibition of hypocotyl elongation of various non-transgenic phy mutants and transgenic *phyA/phyB/phyD/phyE* seedlings. (b) Fluence response curves for the inhibition of hypocotyl elongation of *fhy1/fhl* seedlings expressing PHYE-YFP in constant R light (cR). Asterisks indicate the results of Student's two-tailed heteroscedastic *t*-test analysis (**, $P < 0.01$; ***, $P < 0.0001$). (c) Six-day-old dark-grown transgenic *fhy1/fhl* seedlings expressing PHYE-YFP were exposed to either 0.08 or 0.4 $\mu\text{mol m}^{-2} \text{s}^{-1}$ R light for 6 h before microscopic analysis. R light-induced nuclear accumulation was determined and normalized to the corresponding etiolated control (cD). Error bars indicate \pm SE. (d) Six-day-old dark-grown transgenic *phyB-9* seedlings expressing PHYB-GFP were exposed to either 0.08 or 0.4 $\mu\text{mol m}^{-2} \text{s}^{-1}$ R light for 6 h before microscopic analysis. R light-induced nuclear accumulation was determined and normalized to the corresponding etiolated control (cD). Error bars indicate \pm SE. (e) PHYE-YFP is detected as a homodimer in etiolated or R light-treated seedlings. Native gel analysis of non-denatured extracts prepared from *phyA/phyB/phyD* mutant seedlings expressing PHYE-YFP grown at 20°C in the dark for 7 d (D); under the same conditions, but exposed to 3 h (3), 6 h (6) or 24 h (24) R light (25 $\mu\text{mol m}^{-2} \text{s}^{-1}$) just before harvest, or under 7 d R light (cR). Extracts were fractionated on 4–20% gradient native polyacrylamide gel electrophoresis (PAGE) gels, blotted and probed with anti-GREEN FLUORESCENT PROTEIN (GFP) antibody. Asterisk indicates the positions of PHYE dimers. All experiments were repeated three times.

results clearly demonstrate that, pairwise, the truncated and full-length phyC, phyD and phyE photoreceptors regulate the same responses, which, in turn, display similar fluence rate dependences. Close inspection of the data also reveal that the responses regulated by PHYE-YFP and N-terminal PHYE-YFP are not only initiated, but also saturated, at much lower R light intensities

than those controlled by PHYC and PHYD. The data shown in Fig. 4(b) indicate that 8–10 times over-expressed PHYE could contribute to signaling at very low fluences of R light. The data reported by Hennig *et al.* (2002) also demonstrate a similar role for native phyE in controlling seed germination, and thus provide further support for the conclusion above. Microarray analysis has

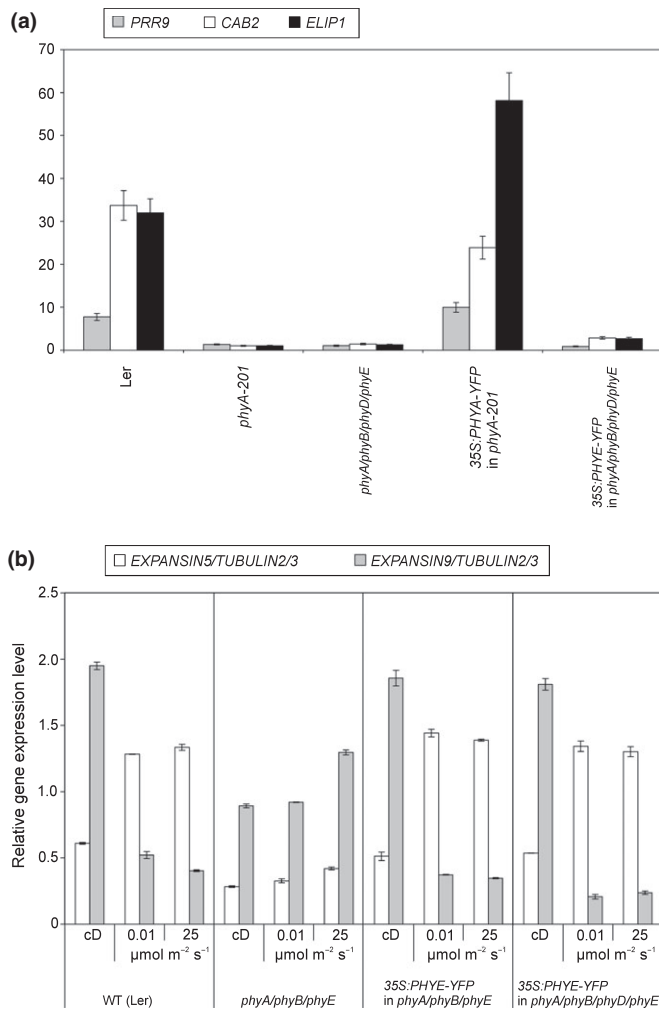


Fig. 5 PHYE regulates gene expression independent of other phytochromes in *Arabidopsis thaliana*. (a) Expression of *PRR9*, *CAB2* and *ELIP1* is not induced by a short red (R) pulse in seedlings expressing PHYE. Four-day-old etiolated seedlings were illuminated with a 30-s R light pulse to generate 1.9% P_{fr} . After the light treatment, seedlings were transferred back to darkness for 1 h, and then samples were collected for RNA isolation. (b) R light changes the transcript level of *EXPANSIN5* and *EXPANSIN9* genes in seedlings expressing PHYE. Seedlings were grown under either 0.01 or 20 $\mu\text{mol m}^{-2} \text{s}^{-1}$ of R light for 4 d or kept in darkness (cD) before sample collection. Gene expression levels were determined by quantitative reverse transcription-polymerase chain reaction (qRT-PCR), and the data obtained were normalized to *TUBULIN2/3* levels. Error bars indicate \pm SE.

documented that *phyA* plays a prominent role in launching the R light-induced transcriptional cascade(s) (Tepperman *et al.*, 2006), and the same authors showed that R light is ineffective in inducing the transcription of key regulatory transcription factors in the *phyA/phyB* mutant (Tepperman *et al.*, 2004). These data suggest that the molecular mechanism by which PHYE regulates gene expression is substantially different from that used by *phyA* and *phyB*. Independent of the molecular mechanism mediating the *phyE*-controlled signaling cascade, our data show that R light-induced or -repressed transcription of *EXPANSIN5* and *EXPANSIN9*, respectively, is reconstituted in the PHYE-YFP-

complemented mutant lines (Fig. 5b), and this process does not require functional *phyB* and *phyD*. PHYE593-YFP-DD-NLS, similar to PHYE-YFP, is also active in controlling the transcription of selected genes in the complemented transgenic plants (Fig. S8). As for the early steps of R light-induced signaling, it is generally accepted that light quality- and quantity-dependent translocation of *phyA* (Hiltbrunner *et al.*, 2005) and *phyB* (Kircher *et al.*, 1999) into the nucleus is critical and rate limiting. The import of *phyA* into the nucleus is mediated by FHY1/FHL (Genoud *et al.*, 2008). Here, we show that the fluence rate dependence of physiological responses and the nuclear accumulation of the PHYE-YFP fusion protein display excellent correlation. The accumulation of PHYE-YFP in the nucleus is induced by extremely low intensities of R light in WT, *phyA/phyB/phyD* and *fhy1/fhl* mutant seedlings, and saturates at low intensities of R light (Fig. 4c). These data demonstrate that translocation of PHYE-YFP into the nucleus is not regulated by FHY1/FHL, and obligate heterodimerization of *phyE* with *phyB* (Clack *et al.*, 2009) is dispensable for the regulation of this process, but does not exclude the possibility that *phyB/phyE* heterodimers are also imported into the nucleus *in planta*. The same authors also reported that over-expressed PHYE-MYC6 fusion protein is monomeric and is assumed to be inactive in R/FR light-induced signaling. By contrast, we detected PHYE-YFP mainly as homodimers in the transgenic *phyA/phyB/phyD* mutant, in both etiolated and R light-treated seedlings. We speculate that the apparent contradiction could be the result of the increased stability of PHYE-YFP homodimers relative to PHYE-MYC6 or, alternatively, the MYC6 tag may destabilize the inherently weak *phyE* homodimers. We also note that the abundance of the PHYE-YFP homodimers (Fig. 4e) appears to be more strongly reduced by extended irradiation of R light when compared with the total amount of PHYE-YFP (Fig. S6a,b). Whether the accelerated degradation of *phyE* homodimers plays a role in the saturation of *phyE*-controlled responses at low fluence rates of R light remains to be elucidated. Notwithstanding these as yet unresolved issues, our data demonstrate that over-expressed PHYE-YFP forms homodimers, *phyE*-controlled physiological responses saturate at low fluence rates of R light, and the import of PHYE-YFP homodimers into the nucleus is mediated by as yet unknown molecular machinery that differs substantially from that described for *phyA*. When compared with *phyE*, the nuclear import of *phyB* displays a different fluence rate dependence, in that it is not saturated at low intensities of R light, and it has been shown that PIFs may be involved in the mediation of translocation of *phyB* into the nucleus (Pfeiffer *et al.*, 2012). Thus, it is tempting to speculate that the molecular mechanism required for R-induced accumulation of *phyE* and *phyB* in the nucleus is also different; however, validation of this hypothesis requires additional molecular and genetic evidence.

PhyB P_{fr} localized in the nucleus is associated with nuclear complexes, termed nuclear bodies, whose size and number appear to be modulated by the intensity and duration of exposure to R light (Kircher *et al.*, 1999; Chen *et al.*, 2004; Van Buskirk *et al.*, 2012). It has been reported by Kircher *et al.* (2002) that PHYB-GFP, PHYC-GFP and PHYE-GFP fusion proteins are associated

with stable NBs in white light-grown transgenic Ws seedlings. Here, we report that we were unable to detect late, stable NBs associated with the truncated PHYC, PHYD and PHYE-YFP fusion proteins (Table S4). By contrast, we observed the formation of such PHYC-YFP and PHYE-YFP NBs in transgenic seedlings expressing the native phyB photoreceptor, but not in transgenic *phyA/phyB/phyD* mutants, independent of the R light treatments applied (Table S4). These data suggest that the formation of stable phyC and phyE NBs under extended R irradiation requires either phyB or active signaling by phyB. We assume that the formation of stable PHYD-YFP NBs requires signaling by other photoreceptor(s), as it can only be detected in white light (Table S4). The formation of early, transient phyC, phyD and phyE NBs displays a more complex pattern. It appears that R light only induces the formation of transient PHYE593-YFP-DD-NLS NBs in the *phyA/phyB/phyE* mutant background (Figs S3, S5, S7). With regard to the R light-induced formation of transient PHYC-YFP and PHYE-YFP NBs, we have shown that such NBs can be detected in the WT Ws background. We have also demonstrated that native phyB is dismissible for the formation of transient phyE NBs, but the absence of both native phyB and phyD prevents the formation of such PHYE-YFP NBs (Table S4). By contrast, we found that PHYD-YFP fails to form R light-induced transient NBs in any genetic background investigated. On the basis of these data, we tentatively conclude that the formation of these transient NBs might be associated with heterodimerization, but this is dismissible, at least for PHYE-YFP signaling.

Taken together, our data suggest that PHYC-YFP, PHYD-YFP and PHYE-YFP fusion proteins, as well as their truncated N-terminal derivatives, are biologically active in the modulation of R light-regulated photomorphogenesis in the specific genetic backgrounds tested. The transgenic plants generated could be useful to gain more insight into the molecular mechanism by which these type II phytochromes signal. Furthermore, independent of the precise mode of action, our data collectively suggest that the truncated PHYC, PHYD and PHYE photoreceptors function as R/FR reversible switches *in planta*. N-terminal fragments of phyB have been successfully used to control cellular signaling processes in a R/FR reversible fashion in bacteria, yeast and mammalian cells (for a review, see Wang *et al.*, 2012). Thus, we believe that it could be advantageous to explore the applicability of our chimeric photoreceptors to synthetic biology research approaches.

Acknowledgements

Work in Hungary was supported by grants OTKA 81399 and TAMOP-4.2.2.A-11/1/KONV-2012-0035 and, in the UK, by SULSA Professorial grant to F.N. Research in Germany was supported by grants SFB 592 and 746 to E.S. and SFB 592 to S.K., whereas work in Spain was supported by Marie Curie IRG-046568 and BIO2006-09254 and BIO2009-07675 grants to E.M. Work in the USA was supported by National Science Foundation Grant (IOS-0920766) to R.A.S.

References

- Aukerman M, Hirschfeld M, Wester L, Weaver M, Clack T, Amasino RM, Sharrock RA. 1997. A deletion in the *PHYD* gene of the *Arabidopsis* Wassilewskija ecotype defines a role for phytochrome D in red/far-red light sensing. *Plant Cell* 9: 1317–1326.
- Bauer D, Viczian A, Kircher S, Nobis T, Nitschke R, Kunkel T, Panigrahi KC, Adam E, Fejes E, Schafer E *et al.* 2004. Constitutive photomorphogenesis 1 and multiple photoreceptors control degradation of phytochrome interacting factor 3, a transcription factor required for light signaling in *Arabidopsis*. *Plant Cell* 16: 1433–1445.
- Chen M, Chory J, Fankhauser C. 2004. Light signal transduction in higher plants. *Annual Review of Genetics* 38: 87–117.
- Chen M, Tao Y, Lim J, Shaw A, Chory J. 2005. Regulation of phytochrome B nuclear localization through light-dependent unmasking of nuclear-localization signals. *Current Biology* 15: 637–642.
- Clack T, Shokry A, Moffet M, Liu P, Faul M, Sharrock RA. 2009. Obligate heterodimerization of *Arabidopsis* phytochromes C and E and interaction with the PIF3 basic helix-loop-helix transcription factor. *Plant Cell* 21: 786–799.
- Clough SJ, Bent AF. 1998. Floral dip: a simplified method for *Agrobacterium*-mediated transformation of *Arabidopsis thaliana*. *Plant Journal* 16: 735–743.
- Demarsy E, Fankhauser C. 2009. Higher plants use LOV to perceive blue light. *Current Opinion in Plant Biology* 12: 69–74.
- Devlin PF, Patel SR, Whitelam GC. 1998. Phytochrome E influences internode elongation and flowering time in *Arabidopsis*. *Plant Cell* 10: 1479–1487.
- Fankhauser C, Chen M. 2008. Transposing phytochrome into the nucleus. *Trends in Plant Science* 13: 596–601.
- Genoud T, Schweizer F, Tscheuschler A, Debrieux D, Casal JJ, Schafer E, Hiltbrunner A, Fankhauser C. 2008. FHY1 mediates nuclear import of the light-activated phytochrome A photoreceptor. *PLoS Genetics* 4: e1000143.
- Hennig L, Stoddart WM, Dieterle M, Whitelam GC, Schäfer E. 2002. Phytochrome E controls light-induced germination of *Arabidopsis*. *Plant Physiology* 128: 194–200.
- Hiltbrunner A, Tscheuschler A, Viczian A, Kunkel T, Kircher S, Schafer E. 2006. FHY1 and FHL act together to mediate nuclear accumulation of the phytochrome A photoreceptor. *Plant and Cell Physiology* 47: 1023–1034.
- Hiltbrunner A, Viczian A, Bury E, Tscheuschler A, Kircher S, Toth R, Honsberger A, Nagy F, Fankhauser C, Schäfer E. 2005. Nuclear accumulation of the phytochrome A photoreceptor requires FHY1. *Current Biology* 15: 2125–2130.
- Hirschfeld M, Tepperman JM, Clack T, Quail PH, Sharrock RA. 1998. Coordination of phytochrome levels in *phyB* mutants of *Arabidopsis* as revealed by apoprotein-specific monoclonal antibodies. *Genetics* 149: 523–535.
- Kircher S, Gil P, Kozma-Bognar L, Fejes E, Speth V, Hüsselstein-Müller T, Bauer D, Adam E, Schäfer E, Nagy F. 2002. Nucleocytoplasmic partitioning of the plant photoreceptors phytochrome A, B, C, D, and E is regulated differentially by light and exhibits a diurnal rhythm. *Plant Cell* 14: 1541–1555.
- Kircher S, Kozma-Bognar L, Kim L, Adam E, Harter K, Schäfer E, Nagy F. 1999. Light quality-dependent nuclear import of the plant photoreceptors phytochrome A and B. *Plant Cell* 11: 1445–1456.
- Lorain S, Allen T, Duek PD, Whitelam GC, Fankhauser C. 2008. Phytochrome-mediated inhibition of shade avoidance involves degradation of growth-promoting bHLH transcription factors. *Plant Journal* 53: 312–323.
- Matsushita T, Mochizuki N, Nagatani A. 2003. Dimers of the N-terminal domain of phytochrome B are functional in the nucleus. *Nature* 424: 571–574.
- Monte E, Alonso JM, Ecker JR, Zhang Y, Li X, Young J, Austin-Phillips S, Quail PH. 2003. Isolation and characterization of phyC mutants in *Arabidopsis* reveals complex crosstalk between phytochrome signaling pathways. *Plant Cell* 15: 1962–1980.
- Nagy F, Schäfer E. 2002. Phytochromes control photomorphogenesis by differentially regulated, interacting signaling pathways in higher plants. *Annual Review of Plant Biology* 53: 329–355.
- Neff MM, Chory J. 1998. Genetic interactions between phytochrome A, phytochrome B, and cryptochrome 1 during *Arabidopsis* development. *Plant Physiology* 118: 27–35.

- Oka Y, Matsushita T, Mochizuki N, Suzuki T, Tokutomi S, Nagatani A. 2004. Functional analysis of a 450-amino acid N-terminal fragment of phytochrome B in Arabidopsis. *Plant Cell* 16: 2104–2116.
- Palágyi A, Terecskei K, Adam E, Kevei E, Kircher S, Merai Z, Schafer E, Nagy F, Kozma-Bognar L. 2010. Functional analysis of amino-terminal domains of the photoreceptor phytochrome B. *Plant Physiology* 153: 1834–1845.
- Park E, Park J, Kim J, Nagatani A, Lagarias JC, Choi G. 2012. Phytochrome B inhibits binding of phytochrome-interacting factors to their target promoters. *Plant Journal* 72: 537–546.
- Pfeiffer A, Kunkel T, Hiltbrunner A, Neuhaus G, Wolf I, Speth V, Adam E, Nagy F, Schafer E. 2009. A cell-free system for light-dependent nuclear import of phytochrome. *Plant Journal* 57: 680–689.
- Pfeiffer A, Nagel MK, Popp C, Wust F, Bindics J, Viczian A, Hiltbrunner A, Nagy F, Kunkel T, Schafer E. 2012. Interaction with plant transcription factors can mediate nuclear import of phytochrome B. *Proceedings of the National Academy of Sciences, USA* 109: 5892–5897.
- Reed JW, Nagpal P, Poole DS, Furuya M, Chory J. 1993. Mutations in the gene for the red far-red light receptor phytochrome B alter cell elongation and physiological responses throughout Arabidopsis development. *Plant Cell* 5: 147–157.
- Rizzini L, Favory JJ, Cloix C, Faggionato D, O'Hara A, Kaiserli E, Baumeister R, Schafer E, Nagy F, Jenkins GI *et al.* 2011. Perception of UV-B by the Arabidopsis UVR8 protein. *Science* 332: 103–106.
- Rockwell NC, Lagarias JC. 2006. The structure of phytochrome: a picture is worth a thousand spectra. *Plant Cell* 18: 4–14.
- Sharrock RA, Clack T. 2004. Heterodimerization of type II phytochromes in Arabidopsis. *Proceedings of the National Academy of Sciences, USA* 101: 11500–11505.
- Sokolova V, Bindics J, Kircher S, Adam E, Schafer E, Nagy F, Viczian A. 2012. Missense mutation in the amino terminus of phytochrome A disrupts the nuclear import of the photoreceptor. *Plant Physiology* 158: 107–118.
- Tepperman JM, Hudson M, Khanna R, Zhu T, Chang SH, Wang X, Quail PH. 2004. Expression profiling of *phyB* mutant demonstrates substantial contribution of other phytochromes to red-light-regulated gene expression during seedling de-etiolation. *Plant Journal* 38: 725–739.
- Tepperman JM, Hwang Y-S, Quail PH. 2006. *phyA* dominates in transduction of red-light signals to rapidly responding genes at the initiation of Arabidopsis seedling de-etiolation. *Plant Journal* 48: 728–742.
- Van Buskirk EK, Decker PV, Chen M. 2012. Photobodies in light signaling. *Plant Physiology* 158: 52–60.
- Viczian A, Adam E, Wolf I, Bindics J, Kircher S, Heijde M, Ulm R, Schafer E, Nagy F. 2012. A short amino-terminal part of Arabidopsis phytochrome A induces constitutive photomorphogenic response. *Molecular Plant* 5: 629–641.
- Viczian A, Kircher S. 2010. Luciferase and green fluorescent protein reporter genes as tools to determine protein abundance and intracellular dynamics. *Methods in Molecular Biology* 655: 293–312.
- Wagner D, Fairchild CD, Kuhn RM, Quail PH. 1996. Chromophore-bearing NH₂-terminal domains of phytochromes A and B determine their photosensory specificity and differential light lability. *Proceedings of the National Academy of Sciences, USA* 93: 4011–4015.
- Wang X, Chen X, Yang Y. 2012. Spatiotemporal control of gene expression by a light-switchable transgene system. *Nature Methods* 9: 266–269.
- Wolf I, Kircher S, Fejes E, Kozma-Bognar L, Schafer E, Nagy F, Adam E. 2011. Light-regulated nuclear import and degradation of Arabidopsis phytochrome-A N-terminal fragments. *Plant and Cell Physiology* 52: 361–372.
- Yamaguchi R, Nakamura M, Mochizuki N, Kay SA, Nagatani A. 1999. Light-dependent translocation of a phytochrome B-GFP fusion protein to the nucleus in transgenic Arabidopsis. *Journal of Cell Biology* 145: 437–445.
- Yu X, Liu H, Klejnot J, Lin C. 2010. The cryptochrome blue light receptors. *Arabidopsis Book* 8: e0135.

Supporting Information

Additional supporting information may be found in the online version of this article.

Fig. S1 Schematic illustration of the domain structures of the native Arabidopsis phytochrome proteins and chimeric PHYC, D and E N-terminal fusion proteins used in this study.

Fig. S2 Immunoblot analysis of the expression level of the various PHYC-YFP fusion proteins compared with the native phyC in Ws wild-type.

Fig. S3 Intracellular localization of the various PHYC-YFP fusion proteins determined in transgenic *phyC/phyD* seedlings.

Fig. S4 Immunoblot analysis of the expression level of the various PHYD-YFP fusion proteins compared with the native phyD in Ler wild-type seedlings.

Fig. S5 Intracellular localization of the various PHYD-YFP fusion proteins determined in transgenic *phyA/phyB/phyD* seedlings.

Fig. S6 Immunoblot analysis of the expression level of the various PHYE-YFP fusion proteins compared with the native phyE in Ler wild-type seedlings.

Fig. S7 Intracellular localization of the various PHYE-YFP fusion proteins determined in transgenic *phyA/phyB/phyE* seedlings.

Fig. S8 PHYE regulates red light-induced gene repression.

Table S1 Oligonucleotides used in this study

Table S2 Summary of the generated transgenic lines and references to the mutant backgrounds used

Table S3 Comparison of endogenous and transgenic PHYC, PHYD and PHYE protein levels in etiolated seedlings calculated on immunoblot assays

Table S4 Red light-dependent formation of nuclear bodies

Please note: Wiley-Blackwell are not responsible for the content or functionality of any supporting information supplied by the authors. Any queries (other than missing material) should be directed to the *New Phytologist* Central Office.

Author Query Form

Journal: NPH

Article: 12364/2013-15307

Dear Author,

During the copy-editing of your paper, the following queries arose. Please respond to these by marking up your proofs with the necessary changes/additions. Please write your answers on the query sheet if there is insufficient space on the page proofs. Please write clearly and follow the conventions shown on the attached corrections sheet. If returning the proof by fax do not write too close to the paper's edge. Please remember that illegible mark-ups may delay publication.

Many thanks for your assistance.

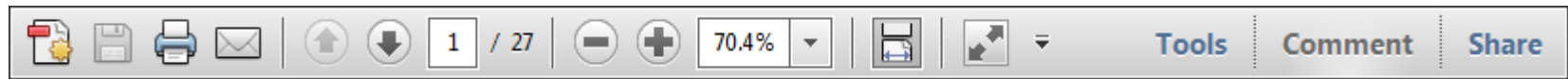
Query reference	Query	Remarks
1	AUTHOR: both phyC/D/E and PHYC/D/E used in this article. Please check that these have been used correctly and consistently throughout this article.	
2	AUTHOR: how many 'additional days'?	
3	AUTHOR: Please give address information for Photometrics: city, state.	
4	AUTHOR: Please give address information for National Institutes of Health: city, state.	
5	AUTHOR: Please give address information for GE Healthcare: town, state (if applicable), and country.	
6	AUTHOR: Please give address information for Thermo Fisher Scientific: town, state (if applicable), and country.	
7	AUTHOR: Please give address information for Fermentas: town, state (if applicable), and country.	
8	AUTHOR: Please check that inserted text 'cD, etiolated control.' is correct.	
9	AUTHOR: Please check that inserted text 'cD, etiolated control.' is correct.	
10	AUTHOR: Please check that inserted text 'cD, etiolated control.' is correct	
11	AUTHOR: '25' not '20' in Fig. 5. Please check.	

USING e-ANNOTATION TOOLS FOR ELECTRONIC PROOF CORRECTION

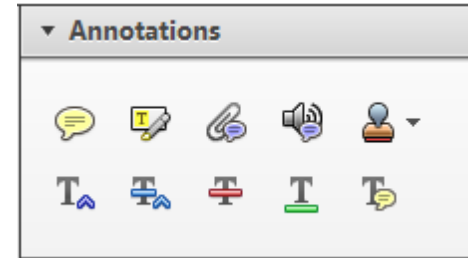
Required software to e-annotate PDFs: Adobe Acrobat Professional or Adobe Reader (version 7.0 or above). (Note that this document uses screenshots from Adobe Reader X)

The latest version of Acrobat Reader can be downloaded for free at: <http://get.adobe.com/uk/reader/>

Once you have Acrobat Reader open on your computer, click on the [Comment](#) tab at the right of the toolbar:



This will open up a panel down the right side of the document. The majority of tools you will use for annotating your proof will be in the [Annotations](#) section, pictured opposite. We've picked out some of these tools below:



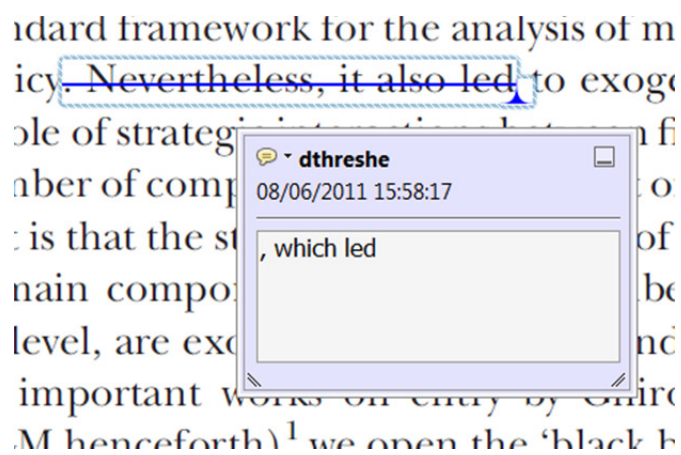
1. Replace (Ins) Tool – for replacing text.



Strikes a line through text and opens up a text box where replacement text can be entered.

How to use it

- Highlight a word or sentence.
- Click on the [Replace \(Ins\)](#) icon in the Annotations section.
- Type the replacement text into the blue box that appears.



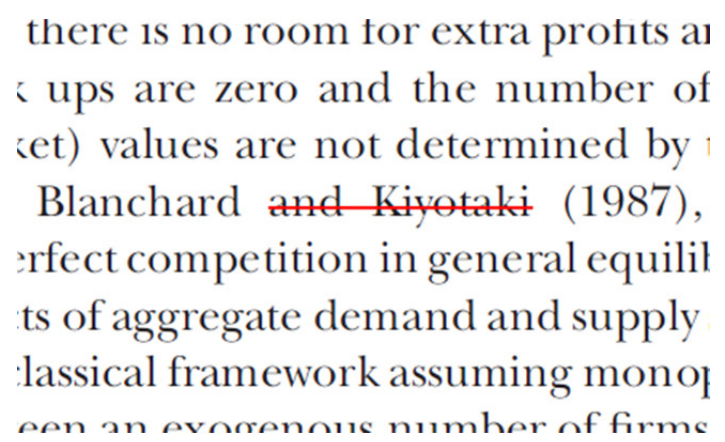
2. Strikethrough (Del) Tool – for deleting text.



Strikes a red line through text that is to be deleted.

How to use it

- Highlight a word or sentence.
- Click on the [Strikethrough \(Del\)](#) icon in the Annotations section.



3. Add note to text Tool – for highlighting a section to be changed to bold or italic.

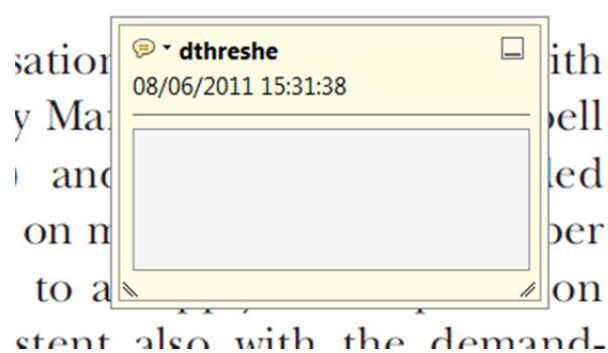


Highlights text in yellow and opens up a text box where comments can be entered.

How to use it

- Highlight the relevant section of text.
- Click on the [Add note to text](#) icon in the Annotations section.
- Type instruction on what should be changed regarding the text into the yellow box that appears.

dynamic responses of mark ups
ent with the **VAR** evidence



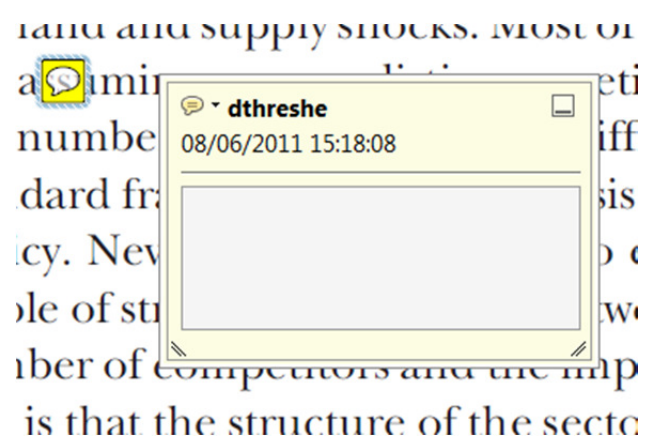
4. Add sticky note Tool – for making notes at specific points in the text.



Marks a point in the proof where a comment needs to be highlighted.

How to use it

- Click on the [Add sticky note](#) icon in the Annotations section.
- Click at the point in the proof where the comment should be inserted.
- Type the comment into the yellow box that appears.



USING e-ANNOTATION TOOLS FOR ELECTRONIC PROOF CORRECTION

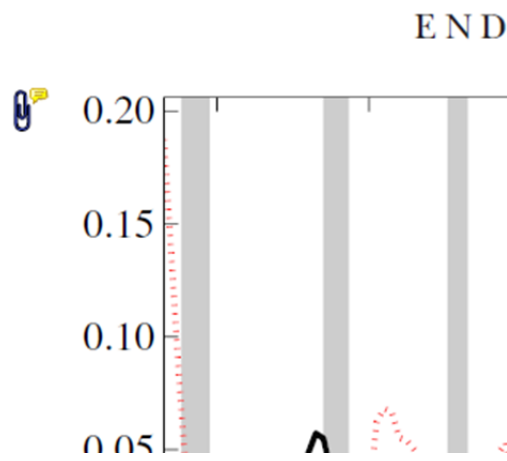
5. Attach File Tool – for inserting large amounts of text or replacement figures.



Inserts an icon linking to the attached file in the appropriate place in the text.

How to use it

- Click on the [Attach File](#) icon in the Annotations section.
- Click on the proof to where you'd like the attached file to be linked.
- Select the file to be attached from your computer or network.
- Select the colour and type of icon that will appear in the proof. Click OK.



6. Add stamp Tool – for approving a proof if no corrections are required.

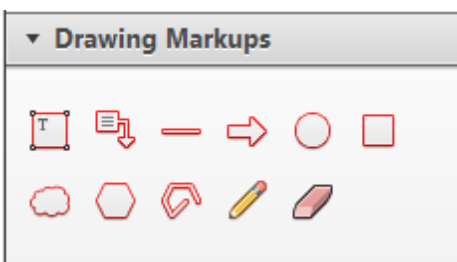


Inserts a selected stamp onto an appropriate place in the proof.

How to use it

- Click on the [Add stamp](#) icon in the Annotations section.
- Select the stamp you want to use. (The [Approved](#) stamp is usually available directly in the menu that appears).
- Click on the proof where you'd like the stamp to appear. (Where a proof is to be approved as it is, this would normally be on the first page).

of the business cycle, starting with the
 on perfect competition, constant return
 production. In this environment goods
 extra profits and the market
 he market. The New-Key
 otaki (1987), has introduced produc
 general equilibrium models with nomin
 ed and supply shocks. Most of this literat

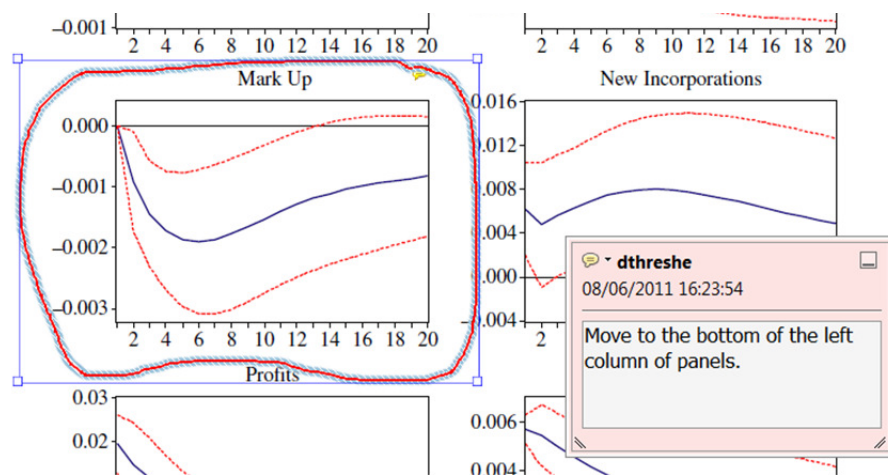


7. Drawing Markups Tools – for drawing shapes, lines and freeform annotations on proofs and commenting on these marks.

Allows shapes, lines and freeform annotations to be drawn on proofs and for comment to be made on these marks..

How to use it

- Click on one of the shapes in the [Drawing Markups](#) section.
- Click on the proof at the relevant point and draw the selected shape with the cursor.
- To add a comment to the drawn shape, move the cursor over the shape until an arrowhead appears.
- Double click on the shape and type any text in the red box that appears.



For further information on how to annotate proofs, click on the [Help](#) menu to reveal a list of further options:

